Contribution from the Department of Chemistry, Rutgers,
The State University of New Jersey, New Brunswick, New Jersey 08903

$Tl_4Re_6X_{12}$ (X = S, Se): Crystal Growth, Structure, and Properties

G. Huan, M. Greaney,† P. P. Tsai, and M. Greenblatt*

Received September 29, 1988

Single crystals of two new phases $Tl_4Re_6S_{12}$ and $Tl_4Re_6Se_{12}$ isostructural with $(Rb,K)_4Re_6Se_{12}$ were synthesized by high-temperature reaction of TlX, Re, and X (X = S, Se). The structure of the selenide was solved by single-crystal X-ray investigation (space group $C2/c$, $R = 0.08$). The structure consists of Re_6Se_8 cluster units interconnected three-dimensionally by four Se and two Se_2 bridges. $Tl_4Re_6S_{12}$ is isostructural with $Tl_4Re_6Se_{12}$. The cell parameters of $Tl_4Re_6S_{12}$ and $Tl_4Re_6Se_{12}$ are $a = 16.653$ (2) Å, $b = 9.574$ (3) Å, $c = 11.816$ (8) Å, $\beta = 90.62$ (2)° and $a = 17.177$ (3) Å, $b = 9.846$ (2) Å, $c = 12.195$ (2) Å, $\beta = 90.71$ (2)°, respectively. $Z = 4$ for both compounds. Physical measurements show that these compounds are semiconducting and diamagnetic, which is consistent with 24 electrons per cluster unit filling the valence band. Bond-order calculations of $Tl_4Re_6Se_{12}$ and other related compounds indicate a Re–Re bond order of 1 in all of the known Re_6X_8 cluster compounds.

Introduction

One of the most interesting aspects of Re^{3+} (d^4) chemistry is that Re atoms tend to form octahedral clusters either in the form of chalcohalides[1-5] or in the form of chalcogenides.[6-12] In the chalcogenides, Re_6X_8 clusters, the basic units of structure, are connected by X or X_2 (X = S, Se) bridging to form a three-dimensional network.

Three types of bridging connections are found in the chalcogenides (Table I):[6-12] (1) single X bridging the clusters, as Se(6) in Figure 1, which is found in $A_4/B_2[Re_6X_8]X_{6/2}$ phases in Table I; (2) four single X and two dichalcogenide X_2 units, as Se(5)–Se(5′) in Figure 1, in $A_4[Re_6X_8]X_{4/2}(X_2)_{2/2}$ compounds in Table I; (3) two X and four X_2 bridging units as in $A_4[Re_6X_8]X_{2/2}(X_2)_{4/2}$ in Table I. The nature of the connectivity is dependent on the size and number of the ternary ions. In general, Se bridges provide more space than S bridges and X_2 bridges provide more space than X bridges. Thus, as the size or the number of the ternary atoms increase, X bridging is partly replaced by X_2 bridging (e.g. $Li_4Re_6S_{11}$ vs $Na_4Re_6S_{12}$) and the selenides become more stable than sulfides ($Rb_4Re_6Se_{12}$ vs $Rb_4Re_6S_{13}$). It seems that there is an optimal size range of the ternary cation for a particular composition, i.e. for $A_4Re_6X_{12}$ when X = S, A = Na^+ or K^+ and when X = Se, A = K^+ or Rb^+. Since Tl^+ is slightly smaller than Rb^+ and it behaves as an alkali-metal cation, we expected the formation of $Tl_4Re_6Se_{12}$. However, since Tl^+ is more polarizing than Rb^+, it was possible that the sulfide analogue might also form. In this paper we report the preparation, crystal structure, and physical properties of the sulfur and selenide $Tl_4Re_6X_{12}$ phases.

Experimental Section

1. Crystal Growth. All the chemicals used in this study were of reagent grade or higher.

$Tl_4Re_6Se_{12}$ single crystals were prepared according to the following reaction:

$$4TlSe + 6Re + 8Se \rightarrow Tl_4Re_6Se_{12}$$

Stoichiometric TlSe, Re (99.997%, Aesar), and Se (99.9%, Aesar) were intimately mixed with about 10 wt % of Tl_2Se, and the mixture was sealed under vacuum ($\sim 10^{-3}$ Torr) in a quartz tube. The mixture was heated in a two-zone furnace (with the charge at the hot end of the quartz tube) slowly to 450 °C and kept at this temperature overnight. Then the temperature was raised to 1150 °C at a rate of 20 °C/h. After being kept at this temperature for 3–4 days, the product was sintered at 900 °C for about 1 week to 10 days and finally cooled down to room temperature in the course of 1 week.

For single crystals of $Tl_4Re_6S_{12}$, the preparation was essentially the same except that extra TlS was used (TlS:Re:S = 5:6:8) and the reaction temperature was 1050 °C. The binary compounds TlS, TlSe, and Tl_2Se were prepared from stoichiometric mixtures of the corresponding elements in evacuated (10^{-4} Torr) quartz tubes at 600 °C for 2 days (the purity of the Tl and S is better than 99.99%; both elements are from Aesar).

2. Elemental Analysis. The chemical composition for both compounds was found by a dc argon plasma emission spectrometer.

Table I. Three Types of Known Ternary Rhenium Chalcogenides

$A_4/B_2[Re_6X_8]X_{6/2}$	ref	$A_4[Re_6X_8]X_{2/2}(X_2)_{4/2}$	ref	$A_4[Re_6X_8]X_{4/2}(X_2)_{2/2}$	ref
$Li_4Re_6S_{11}$	11	$Na_4Re_6S_{12}$	6, 7	$K_2Rb_2Rb_6S_{13}$	12
$Sr_2Re_6S_{11}$	9	$K_4Re_6S_{12}$	6, 7	$Rb_4Re_6S_{13}$	12
$Ba_2Re_6S_{11}$	9	$K_4Re_6Se_{12}$	12	$Cs_4Re_6Se_{13}$	12
$Eu_2Re_6S_{11}$	10	$Rb_4Re_6Se_{12}$	12	$Cs_4Re_6Se_{9.45}Se_{3.55}$	12

Table II. Crystallographic Data for $Tl_4Re_6Se_{12}$

chem formula	$Tl_4Re_6Se_{12}$	Z	4
a	17.177 (3) Å	T	23 °C
b	9.846 (2) Å	λ	0.71069 Å
c	12.195 (2) Å	ρ_{calcd}	9.28 g/cm^3
β	90.71 (2)°	μ	880.3 cm^{-1}
V	2062 (2) Å^3	transmn coeff	0.51–0.99
fw	2882.24	$R(F_o)$	0.081
space group	$C2/c$ (No. 15)	$R_w(F_o^2)$	0.078

3. X-ray Diffraction Data Collection. A multifaceted prismatic crystal was mounted on a glass fiber. The intensity data were collected on an Enraf-Nonius CAD4 automatic four-circle diffractometer at ambient temperature. Data collection parameters are tabulated in Table II. Orientation matrices and unit cell parameters were obtained from 25 centered reflections. Axial photographs and systematic absences hkl ($h + k = 2n + 1$), $h0l$ ($h + l = 2n + 1$), and $0k0$ ($k = 2n + 1$) are consistent with the monoclinic space groups Cc (No. 9) and $C2/c$ (No. 15). E statistics suggested the centrosymmetric space group $C2/c$, and successful solution and refinement of the structure confirmed this choice. Intensity and orientation of three check reflections were monitored every 100 reflections. No significant decay was observed over the course of data collection.

4. Structure Solution and Refinement. The structure was solved by utilizing the SDP single-crystal structure determination package as supplied by Enraf-Nonius. The data were corrected for absorption by an emperical method (ψ), which employs ψ-scan data from high-χ-angle reflections. Standard Lorentz, polarization, and anomalous dispersion corrections were applied to all reflections. The structure was determined by a combination of direct methods (MULTAN) and difference Fourier methods. All atoms were refined anisotropically. Full-matrix least-

† Present address: Exxon Research and Engineering Co., Annandale, NJ 08801.

(1) Opalovskii, A. A.; Fedorov, V. E. Lobkov, E. V.; Erenburg, B. G. *Russ. J. Inorg. Chem. (Engl. Transl.)* **1971**, *16*, 1685.
(2) Leduc, L.; Perrin, A.; Sergent, M. *Acta Crystallogr.* **1983**, *C39*, 1503.
(3) Leduc, L.; Perrin, A.; Sergent, M. *C. R. Acad. Sci., Ser 3* **1983**, *296*, 961.
(4) Leduc, L.; Perrin, A.; Sergent, M.; Le Traon, F.; Pilet, J. C.; Le Troan, A. *Mater. Lett.* **1988**, *3*, 209.
(5) Leduc, L.; Padiou, A.; Perrin, A.; Sergent, M. *J. Less-Common Met.* **1983**, *95*, 73.
(6) Spangenberg, M.; Bronger, W. *Angew. Chem., Int. Ed. Engl.* **1978**, *17*, 368.
(7) Bronger, W.; Spangenberg, M. *J. Less-Common Met.* **1980**, *76*, 73.
(8) Chen, S.; Robinson, W. R. *J. Chem. Soc., Chem. Commun.* **1978**, 879.
(9) Bronger, W.; Miessen, H. J. *J. Less-Common Met.* **1982**, *83*, 29.
(10) Bronger, W.; Miessen, H. J.; Schmitz, D. *J. Less-Common Met.* **1983**, *95*, 275.
(11) Bronger, W.; Miessen, H. J.; Muller, P.; Neugroschel, R. *J. Less-Common Met.* **1985**, *105*, 303.
(12) Bronger, W.; Miessen, H. J.; Neugroschel, R.; Schmitz, D.; Spangenberg, M. *Z. Anorg. Allg. Chem.* **1985**, *525*, 41.

0020-1669/89/1328-2448$01.50/0

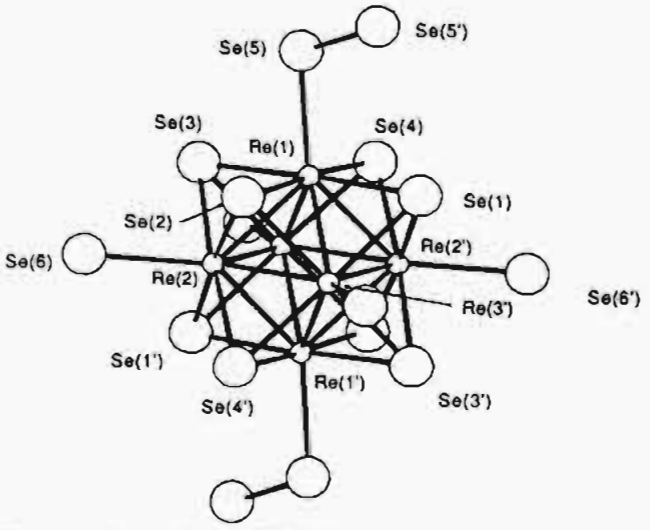

Figure 1. Structural unit of $Tl_4Re_6Se_{12}$.

Table III. Elemental Analysis Data for $Tl_4Re_6Se_{12}$ (X = S, Se)

	% Tl		% Re		% X	
	calcd	found	calcd	found	calcd	found
$Tl_4Re_6S_{12}$	35.24	35.34	48.17	47.56	16.59	17.10
$Tl_4Re_6Se_{12}$	28.36	28.48	38.76	38.02	32.87	33.50

square refinement converged with a final R of 0.081. This high final R value is attributed to our inability to perform adequate absorption correction due to the unusually large linear absorption coefficient of 880 cm^{-1} for this compound.

5. Resistivity Measurement. The resistivity measurement was carried out on a small piece of $Tl_4Re_6Se_{12}$ single crystal by using conventional dc four-probe technique. In the case of $Tl_4Re_6S_{12}$, a sintered pellet was used. Ohmic contacts were made by attaching molten indium ultrasonically.

6. Magnetic Susceptibility Measurements. Susceptibility measurements were performed on single crystals by using a SQUID, Quantum Design magnetometer.

Results and Discussion

1. Single-Crystal Growth of $Tl_4Re_6X_{12}$ (X = S, Se). The methods described in the Experimental Section yield single crystals of both the sulfide and selenide. The crystals grow in a partially melted region of the charge. It appears that addition of the low melting (mp < 500 °C) binaries Tl_2Se, TlSe and Tl_2S, TlS, respectively, to the reaction mixture leads to partial melting of the charge, and crystals of $Tl_4Re_6X_{12}$ (X = S, Se) grow by flux mechanism. The crystals are small ($\sim 1 \times 1 \times 1$ mm^3), silvery, cubelike polyhedra, with a shiny metallic luster. In some experiments, large crystals of $Tl_4Re_6Se_{12}$ with irregular shape were obtained. Figure 2 shows photographs of representative single crystals of $Tl_4Re_6S_{12}$ and $Tl_4Re_6Se_{12}$.

Without the addition of Tl_2Se or excess TlS to the starting materials for both the selenide and sulfide $Tl_4Re_6X_{12}$, no single-crystal growth occurred; only small amounts of Tl_2X and TlX (X = S, Se) were found deposited at the cooler end of the quartz tube (the temperature gradient across the tube is ~50 °C), and polycrystalline $Tl_4Re_6X_{12}$ and ReX_2 were found in the charge zone (hot zone). Thus, excess Tl_2Se or TlS appears to prevent the decomposition of $Tl_4Re_6X_{12}$. Moreover, both Tl_2X and TlX act as a flux, leading to partial solution of the starting materials, which is favorable for crystal growth. The elemental analysis results are listed in Table III.

2. Structure of $Tl_4Re_6Se_{12}$. The atomic coordinates of $Tl_4Re_6Se_{12}$ are shown in Table IV. The basic structural unit of $Tl_4Re_6Se_{12}$ is the Re_6 octahedron inscribed within a cube of selenium atoms, as illustrated in Figure 1. The Re_6Se_8 clusters are interconnected three dimensionally in the solid via diselenide (Se_2) and selenide (Se^{2-}) bridges. Crystallographic inversion centers are found at the body center of the rhenium octahedra as well as at the midpoints of the diselenide bonds. The arrangement of the cluster within the unit cell is identical with that previously reported for $K_4Re_6Se_{12}$ and $Rb_4Re_6Se_{12}$.[12] Selected bond distances and bond angles are sumarized in Table V. The rhenium octahedron is slightly flattened with a Re(1)–Re(1′) distance of 3.708 (3) Å in contrast to the Re(2)–Re(2′) and Re(3)–Re(3′) distances of 3.739 (3) and 3.724 (7) Å, respectively. The average Re–Re distance along the edges of the octahedron is 2.630 Å, which is close to the average Re–Re distances of 2.637 (3) and 2.641 (3) Å found in the K and Rb analogues, respectively.[12] This distance is shorter than that found in Re metal (2.75 Å), implying the existence of Re–Re single bonds along the edges of the rhenium octahedra. The selenium cube is fairly regular with an average Se–Se distance of 3.559 (5) Å and average vertex angles of 90.2(1)°. Each rhenium atom is bonded to four selenium atoms on the face of the selenium cube with an average Re–Se bond distance of 2.519 (4) Å. In addition, each rhenium atom is bonded to a fifth selenium atom, which forms either a selenide or a diselenide bridge to an adjacent rhenium octahedron. The rhenium to diselenide bond distance is 2.582 Å whereas the rhenium to bridging selenide bond is slightly longer: 2.598 (3) Å. The Se(5)–Se(5′) distance of 2.414 (7) Å is similar to those observed for diselenides in the K and Rb analogues: 2.406 (9) and 2.428 (13) Å, respectively.[12] The thallium ions are in irregular interstices within the lattice with Tl(3) in a general position and

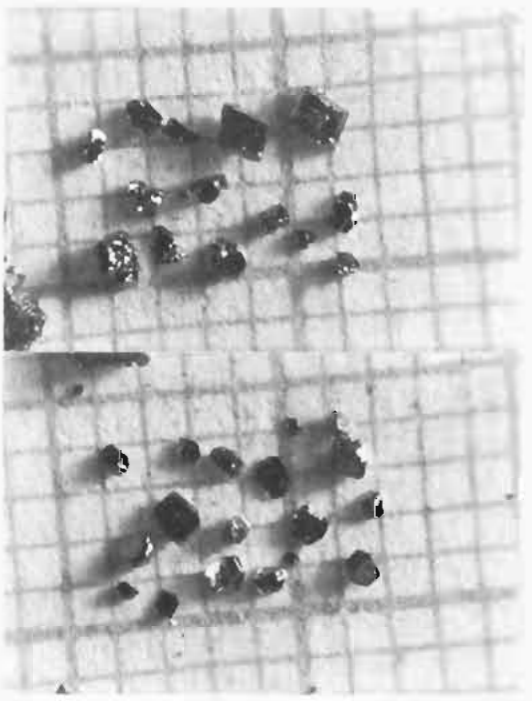

Figure 2. Single crystals of (top) $Tl_4Re_6S_{12}$ and (bottom) $Tl_4Re_6Se_{12}$.

Table IV. Atomic Positional and Thermal Parameters[a] for $Tl_4Re_6Se_{12}$ with Estimated Standard Deviations in Parentheses

atom	x	y	z	B_{eq}, Å^2
Tl(1)	0.0000	0.4130 (6)	0.2500	3.9 (1)
Tl(2)	0.0000	0.7841 (5)	0.2500	2.81 (9)
Tl(3)	0.6032 (2)	0.2514 (3)	0.9850 (2)	2.08 (5)
Re(1)	0.8403 (3)	0.1516 (2)	0.4748 (2)	0.64 (4)
Re(2)	0.7058 (3)	0.1779 (2)	0.3720 (2)	0.65 (4)
Re(3)	0.7900 (1)	0.3943 (2)	0.4193 (2)	0.64 (4)
Se(1)	0.8403 (3)	0.0843 (7)	0.6724 (5)	1.0 (1)
Se(2)	0.7440 (3)	0.4489 (6)	0.0697 (5)	1.0 (1)
Se(3)	0.6684 (4)	0.2753 (7)	0.7229 (5)	1.1 (1)
Se(4)	0.5822 (3)	0.1362 (6)	0.4775 (5)	1.1 (1)
Se(5)	0.9640 (4)	0.9751 (7)	0.9170 (5)	1.1 (1)
Se(6)	0.6434 (3)	0.0866 (6)	0.1918 (5)	1.0 (1)

[a] Anisotropically refined atomic thermal parameters are given in the form of the isotropic equivalent displacement parameter defined as $(4/3)[a^2B(1,1) + b^2B(2,2) + c^2B(3,3) + ab(\cos\gamma)B(1,2) + ac(\cos\beta)B(1,3) + bc(\cos\alpha)B(2,3)]$.

Table V. Selected Interatomic Bond Distances (Å) and Bond Angles (deg) for $Tl_4Re_6Se_{12}$ with Estimated Standard Deviations in Parentheses

	Distances		
Re(1)–Re(1′)	3.708 (3)	Re(2)–Se(4′)	2.530 (4)
Re(2)–Re(2′)	3.739 (3)	Re(1)–Se(5)	2.582 (2)
Re(3)–Re(3′)	3.724 (7)	Re(2)–Se(6′)	2.598 (3)
Re(1)–Re(2)	2.630 (4)	Se(1)–Se(2)	3.536 (6)
Re(1)–Re(3)	2.623 (4)	Se(1)–Se(4)	3.569 (5)
Re(2)–Re(3)	2.638 (5)	Se(2)–Se(3)	3.548 (6)
Re(1)–Se(1)	2.495 (5)	Se(3)–Se(4)	3.592 (5)
Re(1)–Se(2)	2.528 (7)	Se(1)–Se(3′)	3.563 (4)
Re(1)–Se(3)	2.518 (2)	Se(2)–Se(4′)	3.562 (6)
Re(1)–Se(4)	2.535 (2)	Se(3)–Se(1′)	3.563 (4)
Re(2)–Se(2)	2.518 (6)	Se(4)–Se(2′)	3.562 (5)
Re(2)–Se(3′)	2.494 (4)	Se(5)–Se(5′)	2.414 (7)
Re(2)–Se(1)	2.535 (5)		
	Angles		
Re(1)–Re(2)–Re(3)	59.7 (1)	Se(1)–Se(2)–Se(3)	90.1 (2)
Re(2)–Re(3)–Re(1)	60.0 (1)	Se(2)–Se(3)–Se(4)	90.28 (7)
Re(3)–Re(1)–Re(2)	60.3 (1)	Se(3)–Se(4)–Se(1)	88.82 (6)
Re(1)–Re(2)–Re(1′)	89.5 (1)	Se(4)–Se(1)–Se(2)	90.8 (1)
Re(1)–Re(3)–Re(1′)	89.8 (1)	Se(1)–Se(2)–Se(4′)	90.4 (1)
Re(2)–Re(3)–Re(2′)	90.2 (2)	Se(2)–Se(3)–Se(1′)	90.5 (1)
Re(3)–Re(2)–Re(3′)	89.8 (2)	Se(2)–Re(2′)–Se(6′)	93.9 (1)
Re(1)–Se(5)–Se(5′)	106.0 (1)	Se(3)–Re(2′)–Se(6)	91.26 (8)

Table VI. Bond Order Calculation Results for Ternary Rhenium Chalcogenides

compd	PBO/e	BO/e	ref
$Li_4Re_6S_{11}$	0.97	0.98	11
$Eu_2Re_5S_{11}$	0.96	0.98	10
$Ba_2Re_6S_{11}$	0.95	0.97	9
$Na_4Re_6S_{12}$	1.01	1.01	7
$K_4Re_6S_{12}$	0.97	0.99	7
$K_2Rb_2Re_6S_{13}$	0.98	0.99	12
$Rb_4Re_6S_{13}$	1.01	1.00	12
$Cs_4Re_6S_{9.45}Se_{3.55}$	0.97	0.99	12
$Tl_4Re_6Se_{12}$	0.91	0.95	this work
$K_4Re_6Se_{12}$	0.87	0.94	12
$Rb_4Re_6Se_{12}$	0.87	0.93	12
$Cs_4Re_6Se_{13}$	0.89	0.95	12

Tl(1) and Tl(2) on a special 2-fold position. The selenium coordination about Tl(1), Tl(2), and Tl(3) is six, eight, and seven, respectively. Overall, the structure of $Tl_4Re_6Se_{12}$ is isostructural with $K_4Re_6Se_{12}$ and $Rb_4Re_6Se_{12}$.

$Tl_4Re_6S_{12}$ was found to be isostructural with $Tl_4Re_6Se_{12}$ by single-crystal X-ray diffraction studies, with cell constants a = 16.653 (2) Å, b = 9.574 (3) Å, c = 11.816 (8) Å, and β = 90.62 (2)°. No further data collection and structure solution were carried out.

3. Bond-Order Calculation. The structure determination of $Tl_4Re_6Se_{12}$ shows that it is somewhat more regular than the K and Rb analogues. This is also reflected in the results of bond-order calculations. In general, two formulas may be used: Pauling's bond-order calculation (PBO) with $d_n = d_1 - 0.6 \log n$[13] and the Donnay and Allmann's bond-order calculation (BO) with $n = (d_1/d_n)^5$,[14,15] where n is the bond order, d_n is the bond distance of order n, and d_1 is the bond distance of order 1. The value of d_1 can be obtained by the equation $d_1 = 2.750 + 0.6 \log {}^7/_{12} = 2.609$ Å. The calculated results for all structurally characterized ternary rhenium chalcogenides are listed in Table VI.

It is clear that all BO values are very close to 1.00, indicating the existence of two-center two-electron Re–Re bonds in these Re_6 clusters. Furthermore, the bond orders of sulfides are closer to 1.00 than those of selenides, from which we can conclude that the selenides have some matrix effect. Although $Na_4Re_6S_{12}$ was considered by Corbett to be matrix free on the basis of the existence of S/S_2 bridges,[16] in the Se analogues the large deviation of BO (and PBO) from 1.0 is more likely due to overall bonding effects. Finally, one may note that the ternary elements have very little effect on bond order, implying that their function is mainly to provide electrons for charge balance. It is not clear yet why $Tl_4Re_6Se_{12}$ has a bond order (particularly PBO) slightly higher than those of the other analogous selenides listed above.

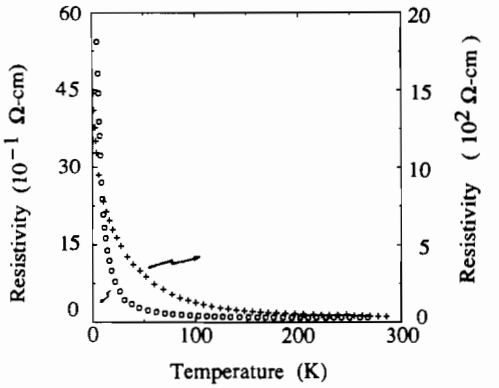

Figure 3. Temperature variation of resistivity for $Tl_4Re_6Se_{12}$ (□) and $Tl_4Re_6S_{12}$ (+).

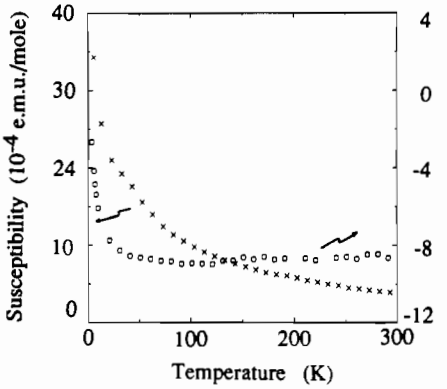

Figure 4. Temperature variation of the magnetic susceptibility for $Tl_{1.8}Re_6Se_{12}$ (×) and $Tl_4Re_6S_{12}$ (□).

4. Chemistry of $Tl_4Re_6X_{12}$ (X = S, Se). Both compounds are stable with respect to air and moisture and can only be dissolved in oxidizing acids. The Tl atoms in the interstitial positions of the lattice have been found to be mobile. They can be partially removed in dilute HCl or I_2/CH_3CN solution at room temperature. The low limit of Tl is $Tl_{1.8}Re_6Se_{12}$; further oxidation results in decomposition. Tl ions can also be replaced by other ions, including alkali-metal ions, Pb, and Cu, via ion-exchange reactions.[17]

5. Physical Properties. Seebeck coefficient measurements show that at room temperature $Tl_4Re_6S_{12}$, $Tl_4Re_6Se_{12}$, and $Tl_{1.8}Re_6Se_{12}$ are p-type semiconductors.

Figure 3 shows the temperature variation of the resistivity measured on a $Tl_4Re_6Se_{12}$ single crystal. As expected, the compound shows semiconducting behavior. The room-temperature resistivity is 0.96×10^{-2} Ω cm, and the thermal activation energy for conduction E_a in the range 36–216 K is 0.012 eV. The room-temperature resistivity of $Tl_4Re_6S_{12}$ is much higher, as shown in Figure 3; the activation energy is 0.20 eV in the range 50–290 K.

Figure 4 shows the temperature dependence of the magnetic susceptibility of $Tl_4Re_6Se_{12}$ measured on single crystals. It shows diamagnetic and almost temperature-independent behavior in the range 300–25 K, and there is a tail at low temperature. The paramagnetic behavior of $Tl_{1.8}Re_6Se_{12}$ measured on a powder sample is shown in Figure 4 as well. μ_{eff} in the temperature range

(13) Pauling, L. *The Nature of the Chemical Bond*, 3rd ed.; Cornell University Press: Ithaca, NY, 1960; pp 400, 403.
(14) Allmann, R. *Monatsh Chemie* **1975**, *106*, 779.
(15) Donnay, G.; Donnay, J. H. *Acta Crystallogr.* **1973**, *B29*, 1417.
(16) Corbett, J. D. *Solid State Chem.* **1981**, *39*, 56.
(17) Huan, G.; Greany, M.; Greenblatt, M. *Mater. Res. Bull.* **1988**, *23*, 905.

32–292 K is 0.95, which gives $S = 1.46$, which is higher than the expected value of 1.1 for 2.2 holes per formula in $Tl_{1.8}Re_6Se_{12}$. The reason for this is not yet clear.

The resistivity and magnetic measurement results are as expected. Each rhenium atom is five-coordinated by selenium atoms in a square-pyramidal geometry (dsp^3), which leaves four d orbitals for each rhenium atom. According to molecular orbital calculations for M_6X_8 clusters,[18-20] there are 24 orbitals per cluster, 12 of which are bonding and 12 are antibonding orbitals with a substantial energy gap between. In $Tl_4Re_6X_{12}$, Tl and Re ions are formally in +1 and +3 oxidation states, respectively,[21] while both X and X_2 are in −2 formal oxidation state. There are 24 electrons per cluster unit, which completely fill the bonding states and leave the antibonding states empty. This explains the semiconducting behavior. The magnitude of the energy gap between bonding and antibonding states is determined by the nature of the bridging groups. Since Se 4p orbitals have greater overlapping ability than S 3p orbitals, it is not surprising that the resistivity and the activation energy of the sulfide are much higher than corresponding values of the Se analogue. Since all the electrons are paired, the diamagnetic behavior of $Tl_4Re_6Se_{12}$ seen in Figure 4 is not unexpected. The upturn of the susceptibility at low temperature found for $Tl_4Re_6Se_{12}$ is probably due to the existence of paramagnetic impurities in the sample. In $Tl_{1.8}Re_6Se_{12}$, holes are expected in the valence band and metallic and Pauli paramagnetic behavior would be anticipated. The source of the observed paramagnetic behavior (Figure 4) is not understood at this time. The magnetic data are consistent with the p-type behavior indicated by the room-temperature Seebeck measurement.

Acknowledgment. We are indebted to Dr. Tom Halbert of Exxon Research and Engineering Co., Annandale, NJ 08801, for helping us with X-ray data collection and structure solution. This research was partially supported by the Office of Naval Research, the National Science Foundation—Solid State Program, under Grants DMR-84-04003, DMR-84-08266, DMR-87-14072, and DMR-87-05620.

Registry No. $Tl_4Re_6Se_{12}$, 117201-42-0; TlSe, 12039-52-0; Re, 7440-15-5; Se, 7782-49-2; Tl_2Se, 15572-25-5; $Tl_4Re_6S_{12}$, 117201-37-3; TlS, 12039-09-7; Tl, 7440-28-0; S, 7704-34-9.

Supplementary Material Available: For $Tl_4Re_6Se_{12}$, Tables SI, SIII, and SIV, listing crystal and refinement data, anisotropic thermal parameters, and nonessential bond distances and angles (7 pages); Table SII, listing observed and calculated structure factors (5 pages). Ordering information is given on any current masthead page.

(18) Cotton, F. A.; Haas, T. E. *Inorg. Chem.* **1964**, *3*, 10.
(19) Bursten, B. E.; Cotton, F. A.; Stanley, G. G. *Isr. J. Chem.* **1980**, *19*, 132.
(20) Hughbanks, T. *Inorg. Chem.* **1986**, *25*, 1492.
(21) Huan, G.; Greaney, M.; Greenblatt, M.; Liang, G.; Croft, M. *Solid State Ionics*, in press.

Contribution from the Department of Chemistry, Rutgers, The State University of New Jersey, New Brunswick, New Jersey 08903, Laboratoire de Chimie Theorique, Universite de Paris-Sud, 91405 Orsay, France, and Department of Chemistry, North Carolina State University, Raleigh, North Carolina 27695-8204

Resistivity Anomalies of the Diphosphate Tungsten Bronze $Cs_{1-x}P_8W_8O_{40}$ (x = 0–0.46) and Its Partially Substituted Phases $Cs_xA_yP_8W_8O_{40}$ (A = Rb, Na) and $CsP_8W_{8-x}Mo_xO_{40}$: Synthesis, Physical Property Measurements, and Band Electronic Structure Calculations

Enoch Wang,[†] Martha Greenblatt,*[,†] Idris El-Idrissi Rachidi,[‡] Enric Canadell,*[,‡] and Myung-Hwan Whangbo*[,§]

Received November 8, 1988

The cesium phosphate tungsten bronze $CsP_8W_8O_{40}$ exhibits a resistivity hump at ~160 K and a resistivity upturn at ~24 K. To understand the origin of these anomalies, we prepared cesium-deficient phases, $Cs_{1-x}P_8W_8O_{40}$, and alkali-metal- and molybdenum-substituted phases, $Cs_xA_yP_8W_8O_{40}$ ($x + y > 1$) and $CsP_8W_{8-x}Mo_xO_{40}$, and measured their electrical resistivities and magnetic susceptibilities. Those results are interpreted on the basis of the tight-binding band electronic structures calculated for the W_4O_{18} chain and the $P_8W_8O_{40}$ lattice.

The phosphate tungsten bronze $CsP_8W_8O_{40}$ contains W_4O_{18} chains (**1**) made of corner-sharing WO_6 octahedra.[1] Those chains

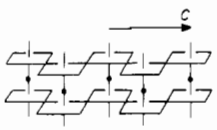

1a

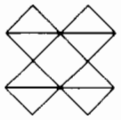

1b

are linked together by P_2O_7 groups (**2**) to form octagonal channels, where Cs atoms reside. The W_4O_{18} chains are isolated in Cs-

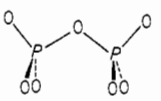

2a

2b

$P_8W_8O_{40}$, so this bronze is expected to be quasi-one-dimensional in electronic properties. Indeed, the electrical transport and magnetic properties of $CsP_8W_8O_{40}$ are consistent with this picture.[2]

The resistivity versus temperature plot of $CsP_8W_8O_{40}$ shows the presence of two resistivity anomalies at ~160 and ~24 K: it is semiconducting from ~760 to ~160 K, metallic between ~160 and ~24 K, and semiconducting below ~24 K. In order to gain insight into the nature of the resistivity hump at ~160

[†] Rutgers University.
[‡] Universite de Paris-Sud.
[§] North Carolina State University.

(1) Goreaud, M.; Labbe, Ph.; Raveau, B. *J. Solid State Chem.* **1985**, *56*, 41.
(2) Wang, E.; Greenblatt, M. *J. Solid State Chem.* **1988**, *76*, 340.

0020-1669/89/1328-2451$01.50/0